4099 b

Acoustic Emission as a Measure of Wood Fracture Energy

Eric N. Landis and Douglas B. Whittaker

Department of Civil & Environmental Engineering, University of Maine USA

Abstract

Recent advances in engineered wood composites are allowing us to further push the load limits of timber used in structural applications. In an effort to better understand failure processes we are applying acoustic emission techniques to examine progressive crack growth parallel to the grain in clear wood specimens loaded for both mode I and mode II fracture. We have developed a technique to estimate the energy released by an acoustic event. By applying basic fracture theory we can determine the bulk fracture energy of the specimen from load-crack length data. A comparison of acoustic energy measurements with bulk fracture energy measurements gives us an idea of how much fracture energy is ultimately measured as acoustic emission energy. This comparison will allow us to apply the technique to laboratory tests of damage growth in larger structures.

1 Introduction

In an effort to better utilize abundant low-grade structural timber we are developing advanced engineered wood composites that strategically reinforced with FRP-composite materials. One such example is a reinforced glue laminated (or glulam) wood beam. In typical glulam fabrication higher quality lumber is required in the zones of high flexural stresses. In the case of tensile stresses, (the most common failure mode of glulam beams), a small amount of FRP reinforcement can change the mode of failure from tension to either shear or compression. In either case, our new failure mode requires us update our understanding of basic wood failure mechanisms because, in effect, we are forcing the wood to work harder than it has had to in the past.

In an effort to better understand and monitor the different failure mechanisms of wood, some small clear wood specimens were loaded to failure while being monitored with an acoustic emission (AE) waveform recording system. Our focus is on mode I, mode II, and mixed mode fracture along the grain, however only the mode I results are presented in this paper. The research objective is to distinguish different energy release mechanisms through analysis of acoustic emission waveforms.

The hypothesis to be tested was as follows. A certain fraction of the energy dissipated by fracture should be detected by an acoustic emission monitoring system. Assuming we can remove effects of material attenuation that alter the acoustic signals as they travel from

source to receiver, then the distribution of energy received by the acoustic emission transducers should be a function of the distribution of the fracture energy released during crack propagation. Our goal then is to measure the distribution of acoustic energy released during a standard fracture test, and to use that information to make inferences on the different fracture mechanisms at work in the material.

In order to test this hypothesis, we assembled a series of clear-grained wood specimens of different moisture contents. By varying the moisture contents, we can vary the fracture toughness of the wood.[1] This variation in fracture toughness becomes the independent variable, while the measured acoustic emission energy release becomes the dependent variable.

The significance of this work is that we presently have difficulty quantifying the damage in a structure in terms of physical characteristics. The idea here is that if we had baseline information on the relationship between acoustic emission energy and the cracks that caused the emissions, we would then be able to quantify damage in terms of crack areas using AE data to estimate that crack area.

2 Experimental Procedure

Our experimental procedure may be summarized as follows. We cut and conditioned to various moisture contents a series clear-grained eastern hemlock (Tsuga Canadensis) specimens. Next, a 7 cm notch was cut along the grain to create a mode I double cantilever configuration. An array of eight acoustic emission sensors was mounted on the specimen as shown in Fig. 1. The AE sensors were connected to a high speed waveform acquisition system (Digital Wave Corp. Fracture Wave Detector). The specimens were

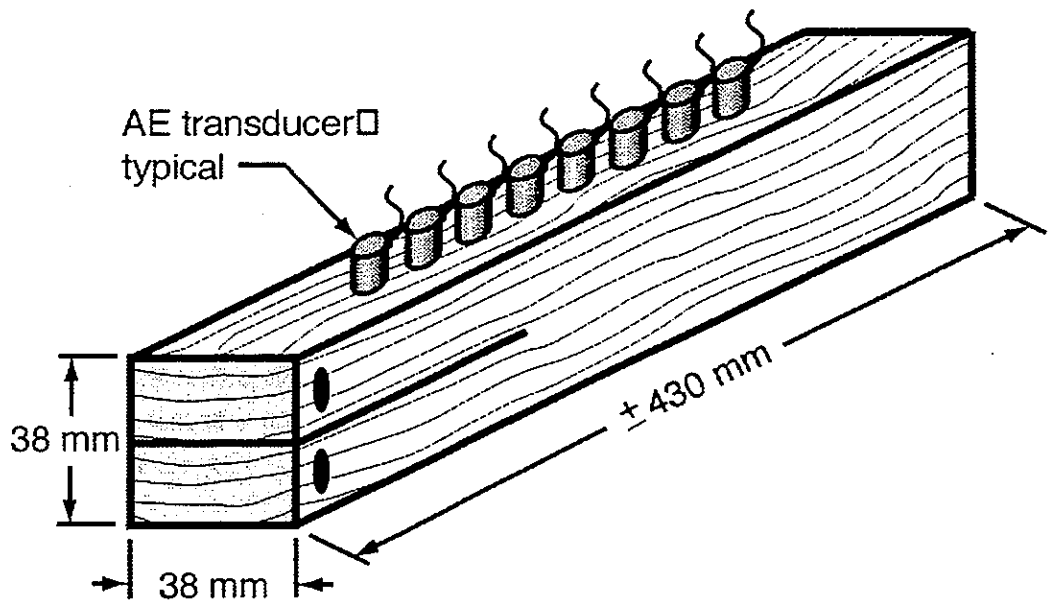

Figure 1. Illustration of Mode I Fracture Specimen.

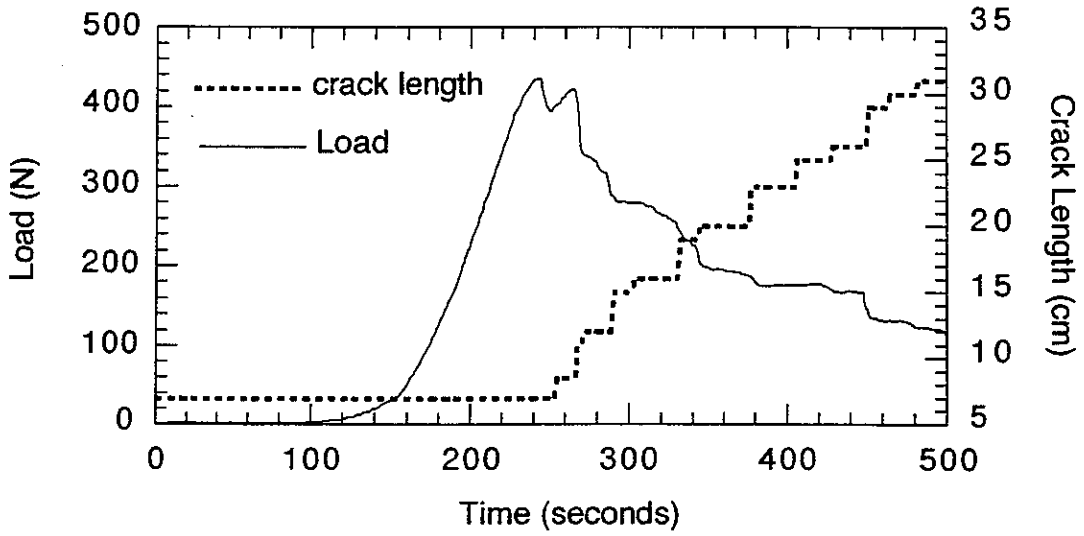

Figure 2. Typical Load and Crack Length Data for Mode I Fracture Test

then loaded under displacement control in a universal testing machine. Load was applied to the specimen through the use of shafts that are pushed into holes drilled through the top and bottom cantilevers. During the test, load, displacement (CMOD), and crack length were all recorded along with the acoustic emission waveform data. A total of 18 specimens were tested at three different moisture contents. Each test produced between 800 and 1200 AE events over the ten minute test length. Prior to each test, the sides of the specimen were coated with a brittle white coating to facilitate observation of crack growth. Crack length was measured using a hand held microscope by comparing the tip of the observed crack with grids drawn on the white surface.

Load and crack length as a function of time are shown for a typical specimen in Fig. 2. The plot shows what we would expect to see. That is that the crack does not start to grow until peak load has been reached.

3 Data Analysis

The two parts to our data analysis are the calculation of bulk fracture energy, and the determination of released acoustic emission energy. These analyses are each detailed below.

3.1 Fracture Analysis

Fracture energy was calculated by monitoring the changes in crack length during loading. Combining the crack length information with the load-deformation curve, the strain energy release rate, G_f, was calculated using the following relationship[2]:

$$G_I = \frac{1}{2B\Delta a}[P_1\delta_1 - P_2\delta_2] \quad (1)$$

where P_1 and δ_1 are load and *CMOD* (Crack Mouth Opening Displacement) at crack length a_1 as shown in Fig. 3, Δa is the change in crack length, a_2 - a_1, and B is the specimen thickness. Typical load and G_I, data are plotted in Fig. 4. It can be seen in the figure that G_I, levels off at a certain point. We can take this leveling off to represent the critical energy release rate G_{IC}, for the material.

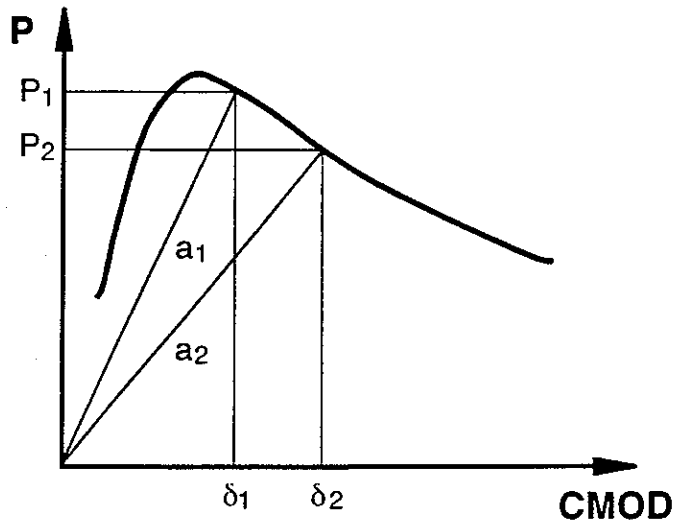

Figure 3. Quantities used in Fracture Energy Calculation

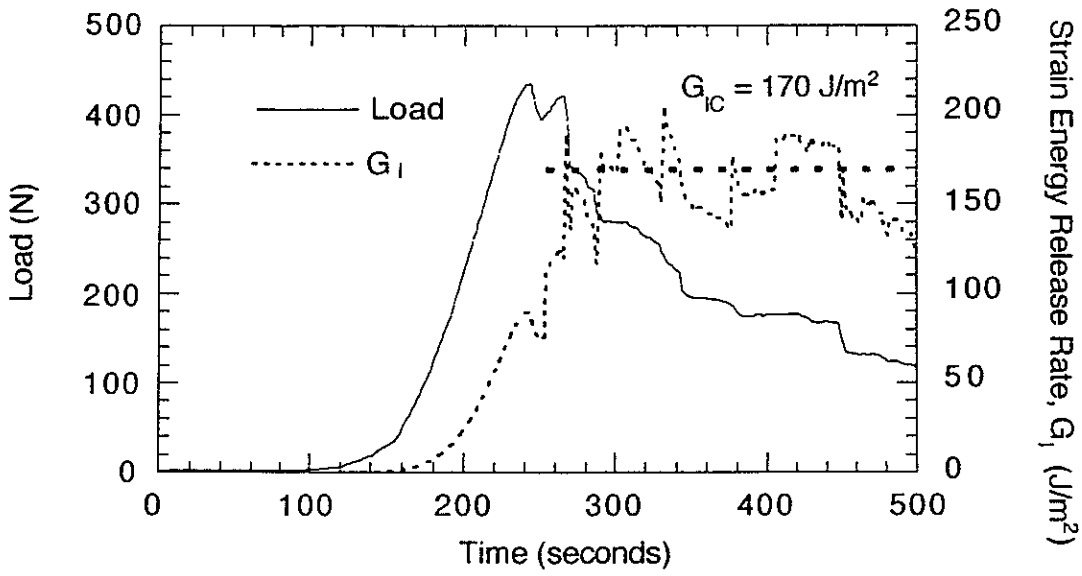

3.2 Acoustic Emission Energy Analysis

The goal of our AE energy analysis was to develop a method by which we could directly measure elastic wave energy. With conventional AE energy analysis, the recorded voltage transient is squared and integrated over time[3]. Although that analysis produces a quantity that is equivalent to energy, the resulting units do not lend themselves to direct comparisons with other energy analyses. As our objective was to compare fracture energy to AE energy, we wanted an analysis technique that resulted in common units (e.g. Joules). The AE energy analysis used in this study is developed below.

The power transport, $\tilde{p}$ of an elastic wave per unit area at a point may be written[4]:

$$\tilde{p}(x,t) = \rho c_L \left(\frac{\partial u}{\partial t}\right)^2 \tag{2}$$

where ρ is the mass density the material, c_L is the longitudinal wave velocity, and u is the particle displacement at the point. We can assume for the moment that we have a harmonic longitudinal wave for which the particle displacement can be written as:

$$u(x,t)) = Ae^{i(kx-\omega t)} \tag{3}$$

where A is the amplitude, k the wave number, and ω the angular frequency. If we substitute (3) into (2) and integrate the real part of the harmonic term over a single period we get average power per unit area of a wave with a single frequency component ω:

$$\tilde{p} = \frac{1}{2}\rho c_L \omega^2 A^2 \tag{4}$$

which has units of energy per unit time per unit area (e.g. J/s m^2). For our broadbanded acoustic emission signals we must add up the contributions of all frequencies. We can do this by integrating our waveform in the frequency domain.

For each AE event, the energy analysis was carried out for the waveform recorded by the transducer closest to the crack tip. This was done to simplify analysis. The waveform from the closest transducer is assumed to have nearly normal incidence. Because the waveforms were recorded using calibrated displacement transducers, we were able to convert these measured voltage transients to displacement transients using the manufacturer's calibration data. This was done using frequency division:

$$U(n) = \frac{V(n)}{T(n)} \tag{5}$$

where $U(n)$, $V(n)$, and $T(n)$ are the frequency representations of the discretely sampled surface displacement, transducer output voltage, and transducer transfer function respectively. n varies from 0 to N, the number of sampled data points (4096 in our case). For a discrete time increment, Δt, the corresponding frequency increment, Δf, is $1/(N\Delta t)$. The corresponding angular frequency increment, $\Delta\omega$ is $2\pi/(N\Delta t)$. After we have determined our frequency representation of the surface displacements, $U(n)$, we can substitute it into equation (4) and integrate over the entire frequency range:

$$\tilde{p} = \sum_{n=0}^{N/2-1} \frac{1}{2}\rho c_L \left(\frac{2\pi n}{N\Delta t}\right)^2 U(n)^2 \tag{6}$$

which simplifies to:

$$\tilde{p} = \frac{2\rho c_L \pi^2}{(N\Delta t)^2} \sum_{n=0}^{N/2-1} n^2 U(n)^2 \tag{7}$$

This equation represents the average power per unit area transmitted by the elastic wave. The resulting power was then multiplied by the time length of the AE signal, and by the area of the propagating elastic wave front.

This energy calculation was done for each of the thousands of AE waveforms recorded throughout the test program. An example of AE energy measurement is shown in Fig. 5, where the cumulative AE energy is plotted as a function of time along with the load for reference purposes.

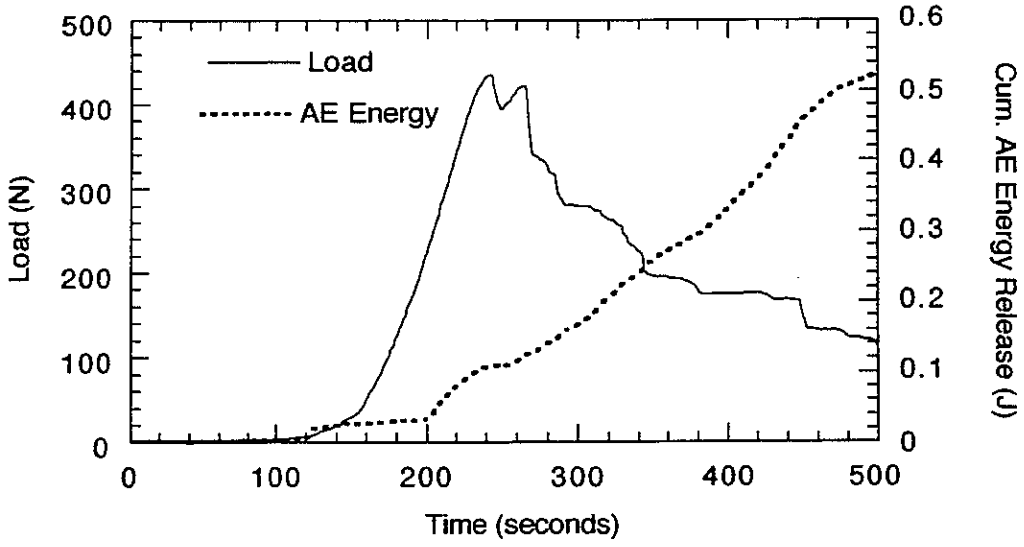

Figure 5. Plot of Typical Load and AE Energy Data.

4 Experimental Results and Discussion

Examination of the plot of Fig. 5 illustrates a number of things. First, very little AE energy is released until just before the peak load has been reached. However the point at which the AE energy increases in rate (at about 200 seconds), is well ahead of when the time at crack is observed to start propagating (about 250 seconds as seen on Fig. 2). There are several explanations for this. First, the resolution of our crack measurement was not fine enough to detect the exact time of crack growth. But another possibility is that there is an internal localization of damage that occurs before the crack actually advances, a phenomenon observed in portland cement-based materials[5].

A second point to observe is the relatively constant rate at which AE energy is released after the crack starts advancing. This can be compared with the relatively constant rate of fracture energy release, as indicated by the moderately constant G_I observed in Fig. 4. As was initially hypothesized, there is likely a relationship between the energy consumed by fracture, and the energy released through acoustic emission.

To make this comparison the first step was to calculate cumulative work of fracture, *W(t)*, by integrating the measured critical energy release rate, G_{IC}, over the crack area created. Or more specifically:

$$W(t) = \int_o^t G_{IC} b a(\tau) d\tau \tag{8}$$

where b is the width of the specimen, $a(t)$ is the crack length at time t.

Plotted in Fig. 6 is the cumulative AE energy along with the cumulative work of fracture. We see in the figure that both AE energy and crack energy are roughly linearly varying quantities with respect to time. A linear fit of both AE and fracture energy after 250 seconds elapsed produces slopes of roughly 0.0095 J/s for the fracture and 0.0014 J/s for the AE. If we compare these two slopes, we could make the conclusion that for this particular specimen fracture energy is being released at almost seven times the rate of AE energy. This procedure was repeated for all specimens tested, and the resulting energy comparison is presented in Fig. 7. The fitted line has a slope of 0.16, indicating that on the average the rate of fracture energy released was over 6 times that of AE.

As to our original hypothesis that AE energy released should be a function of fracture energy, it seems that from our experiments we could conclude that within a range of error it is nearly linear for the specific geometry tested.

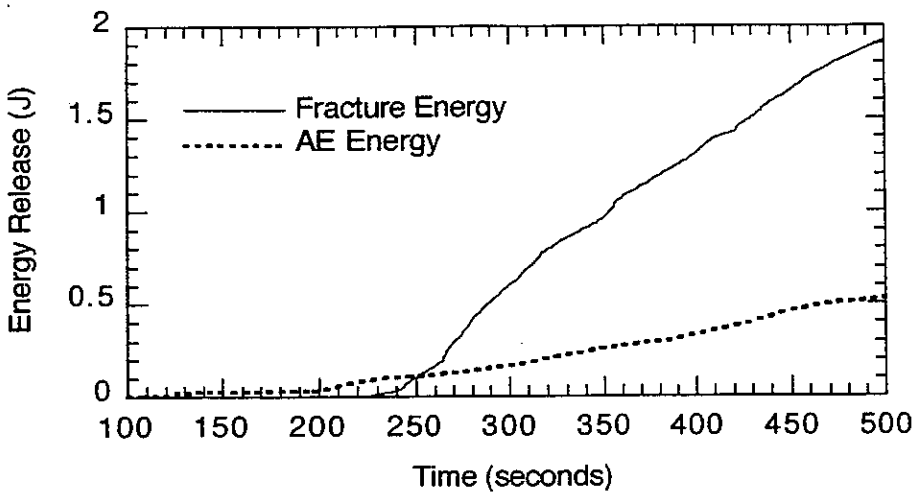

Figure 6. Measured Fracture and AE Energy.

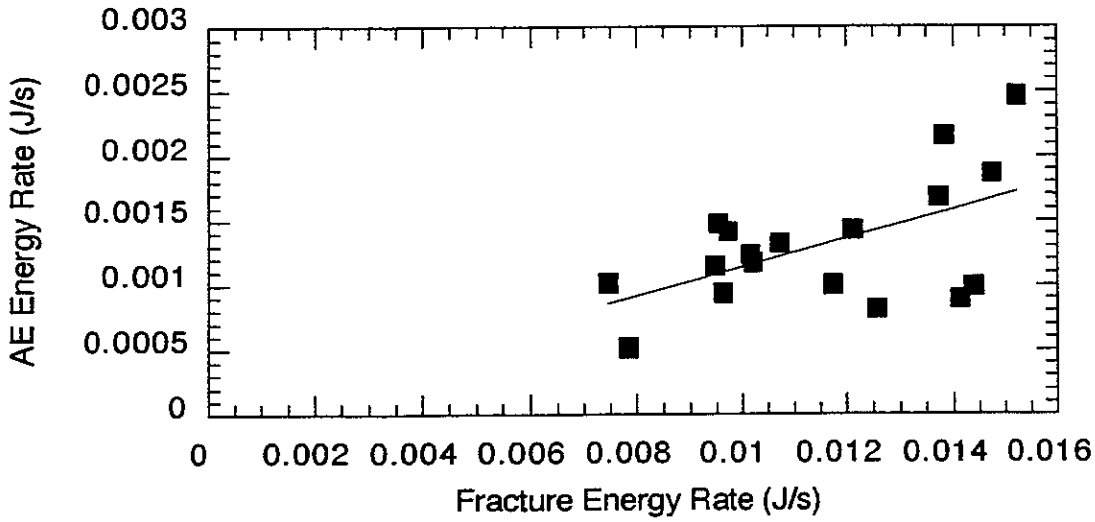

Figure 7. Comparison of Fracture and AE Energy Release Rates.

5 Summary and Conclusions

An experimental program was carried out to compare the energy released by a mode I crack propagating through wood, with the resulting acoustic emission energy that can be monitored with a high speed waveform acquisition system. The fracture energy was calculated by recording the load-CMOD data, as well as the crack length data. Acoustic emission energy release was determined by integrating the instantaneous power of an elastic wave over all frequencies, and multiply the result by the length of the AE waveform. Results of the energy comparison indicate a clear correlation between the fracture energy and the AE energy, which it seems there must be. Future work will be focused on

developing analysis techniques that expand the range of applicability of the analysis technique to a wider range of specimen geometries. Such an expansion could lead to a laboratory technique that is capable of quantifying the internal damage in a structure in terms of the cracks that develop.

6 Acknowledgments

This research was supported by a grant from the U.S. Department of Agriculture Wood Utilization Research Program. Additional support of the Advanced Engineered Wood Composites Center at the University of Maine is gratefully acknowledged.

7 References

1. Bodig, J., and Jayne, B. A. (1982): Mechanics of Wood and Wood Composites. Van Nostrand Reinhold, New York.
2. Daniel, I. M., and Ishai, O. (1994): Engineering Mechanics of Composite Materials. Oxford University Press, New York.
3. Drouillard, T. F. (1987): Introduction to Acoustic Emission Technology. in Nondestructive Handbook, 5, American Society for Nondestructive Testing.
4. Achenbach, J. D. (1973): Wave Propagation in Elastic Solids. North-Holland, Amsterdam.
5. Landis, E. N., and Shah, S. P. (1995): The Influence of Microcracking on the Mechanical Behavior of Cement Based Materials. Advanced Cement Based Materials, 2(3): 105-118.